Reaction in the Al-ZrO₂-C system

ZHENQING WANG*, XIANGFA LIU
*Key Laboratory of Liquid Structure and Heredity of Materials, Ministry of Education,
Shandong University, No.73, Jingshi Road, Jinan, 250061, People's Republic of China*
E-mail: wzhtsing@yahoo.com.cn

The reaction in ball milled Al-ZrO₂-C powders with different ZrO₂/C molar ratios was studied by using DSC, XRD and EPMA. During heating fully milled powders, the Al first reacts with ZrO₂ and carbon simultaneously to form ZrAl₃ and Al₄C₃ phases, which further react with each other at about 896°C, causing the formation of Zr₂Al₃C₅. Then at 1140°C, Zr₂Al₃C₅ reacts with ZrAl₃, producing ZrC and ZrAlC₂ phases. In the un-fully milled powder, only an exothermic reaction between the three starting phases occurs at a higher temperature of about 956°C. Heating Al-ZrO₂-C powders with different ZrO₂/C ratio (*r*) to 1250°C produces different phases in the final aluminum matrix: Al-Al₂O₃-Zr₂Al₃C₅-Al₄C₃ (*r* < 2:5), Al-Al₂O₃-Zr₂Al₃C₅ (*r* = 2:5), Al-Al₂O₃-Zr₂Al₃C₅-ZrC-ZrAlC₂ (2:5 < *r* < 3:5), Al-Al₂O₃-ZrC-ZrAlC₂ (3:5 ≤ *r* ≤ 3:4), Al-ZrAl₃-Al₂O₃-ZrC-ZrAlC₂ (*r* > 3:4). Zr₂Al₃C₅ presents fine platelet morphology, both ZrAlC₂ and ZrC have polygonal shape, ZrAl₃ exhibits flaky morphology at lower temperature, but blocky form at higher temperatures.
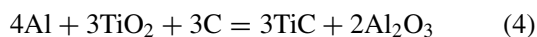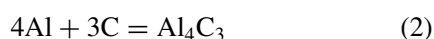© *2005 Springer Science + Business Media, Inc.*

1. Introduction

In situ particulate reinforced metal matrix composites (MMCs) are attractive in the field of advanced materials research due to their excellent mechanical and physical properties, e.g. high specific strength, modulus and good thermal stability. Al₂O₃, TiC, and TiB₂ ceramic particles have been widely examined as reinforcements for *in situ* MMCs [1–7]. During the *in-situ* production of MMCs, these particles are directly formed in metallic matrices through chemical reactions between elements or between elements and compounds. To optimize the processing techniques and properties of final products, it is necessary and important to understand the reaction mechanism responsible for the formation of the reinforcements from starting materials.

Recently, reactions in the Al-TiO₂ [8] and Al-ZrO₂ [9, 10] systems have been investigated to produce *in situ* Al₂O₃ particle reinforced Al composites. However, the inevitable existence of brittle TiAl₃ or ZrAl₃ intermetallic compound in the final aluminum matrix results in the difficulty in controlling products' properties.

By incorporating carbon into the Al-TiO₂ system, we have successfully *in-situ* synthesized TiC and Al₂O₃ ceramic particles in the Al matrix through the direct addition of powder mixtures comprising carbon and TiO₂ into molten aluminum [11, 12]. The following reactions take place during heating the Al-TiO₂-C system:

$$13Al + 3TiO_2 = 3TiAl_3 + 2Al_2O_3 \qquad (1)$$

$$4Al + 3C = Al_4C_3 \qquad (2)$$

$$3TiAl_3 + Al_4C_3 = 3TiC + 13Al \qquad (3)$$

$$4Al + 3TiO_2 + 3C = 3TiC + 2Al_2O_3 \qquad (4)$$

It is predicted by Zheng and Reddy [13] that ZrC is thermodynamically stable in aluminum melt in the temperature range of 933–1600 K (660–1327°C), and thus a desirable reinforcement for aluminum composite. In this paper, the reaction process in the Al-ZrO₂-C system is investigated by using DSC (differential scanning calorimeter), XRD (X-ray diffraction), and EPMA (electron probe microanalysis). The main objective is to evaluate the feasibility of producing ZrC and Al₂O₃ particles reinforced Al matrix composite using this system. It was found, however, that ternary carbides Zr₂Al₃C₅ and ZrAlC₂ form during the heating process and aluminum alloys containing different phases are obtained by varying the ZrO₂/C ratios in the Al-ZrO₂-C system.

2. Experimental procedures

A Powder mixture of 50 g Al (99.0% purity, 200–300 mesh), 18.6 g ZrO₂ (99.5% purity), and *x* g graphite (99.5% purity, 600 mesh) was sealed in a vacuum stainless vial (250 ml) together with 350 g steel balls, then the vial was vacuumized by a rotary vacuum-pump and charged with pure Ar. The value of *x* was varied to obtain different ZrO₂/C molar ratios in the Al-ZrO₂-C system (Table I). Ball milling was performed using a QM-1SP2 planetary-type ball mill at a planetary rotation speed of 450 rev min⁻¹. About 35 mg of the powder mixture milled for predetermined hours was

Sample	x	r	t (h)	Hr (°C/min)	Peak 1 endothermic (°C)	Peak 2 exothermic (°C)	Peak 3 exothermic (°C)	Peak 4 endothermic (°C)	Peak 5 endothermic (°C)
P1	4.39	2:5	8	20	640	680	–	918	–
P2	2.34	3:4	8	20	640	689	–	918	1144
P3	1.81	1:1	8	20	640	689	–	918	1148
P4	2.93	3:5	8	20	640	689	–	918	1144
P5	4.39	2:5	8	5	640	663	–	897	–
P6	2.34	3:4	8	5	640	663	–	896	1141
P7	4.39	2:5	4	20	630	688	845	918	–
P8	2.34	3:4	4	20	640	688	845	918	1140
P9	4.39	2:5	1	20	640	–	–	–	–

r—ZrO_2/C molar ratio, t—Ball milling time, Hr—Heating rate.

Figure 1 DSC traces of P1 and P2 samples.

Figure 2 X-ray diffraction patterns of P1 sample heated to different temperatures by DSC (a) as milled powder; (b) 820°C; (c) 960°C; (d) 1250°C.

Figure 3 X-ray diffraction patterns of P2 sample heated to different temperatures by DSC (a) as milled powder; (b) 820°C; (c) 1000°C; (d) 1250°C.
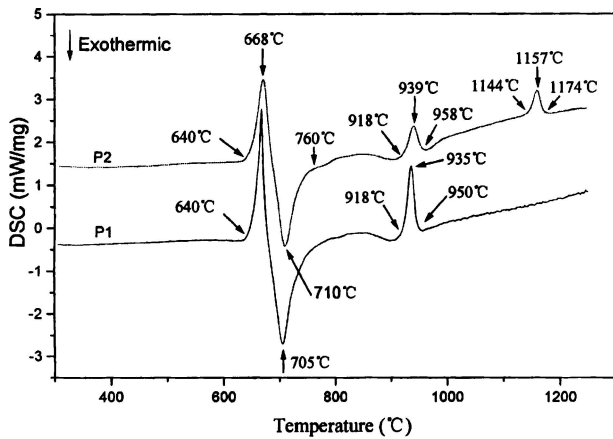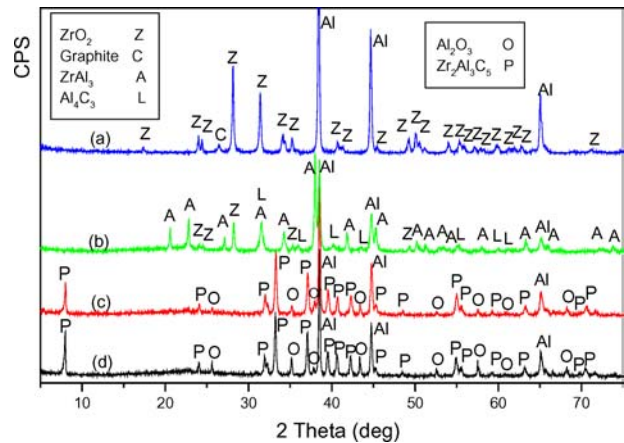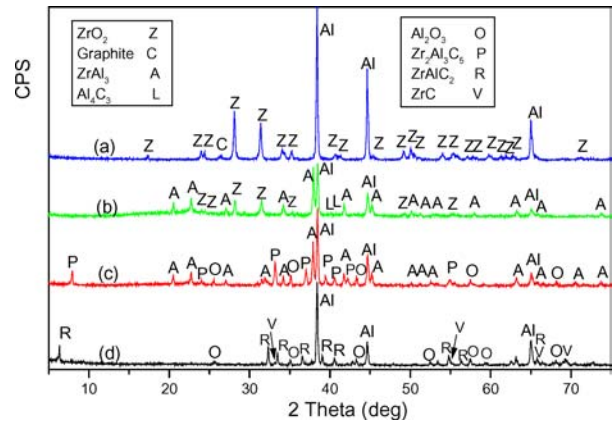
pressed into pellet in a 5 mm die, subsequently heated, under argon atmosphere, in a Netzsch 404 differential scanning calorimeter (DSC), at rates of 5 or 20°C/min, from 25°C to desired temperatures, followed by cooling to ambient temperature at the same rates.

X-ray diffraction (XRD) analysis was carried out using a Rijaku D/max-rB X-ray diffractometer with Cu K_α radiation to identify phases formed in the pellets heated to different temperatures by DSC. The microstructures of the heated pellets were characterized on a JXA-8800R electron probe micro-analyzer (EPMA).

3. Results
3.1. Al-ZrO_2-C powders ball milled for 8 h
DSC traces of P1 and P2 samples are shown in Fig. 1, where the starting, central, and ending temperatures of each reaction peak are indicated. Figs 2 and 3 present the XRD patterns of the P1 and P2 samples heated to different temperatures by DSC, and phases detected are summarized in Table II. Before 1000°C, P1 and P2 samples exhibit similar DSC peaks (peak 1, 2 and 4), but the endothermic peak starting at 1144°C (peak 5) in P2 is absent in P1 specimen.

It is clear that peak 1, which is closely followed by a large exothermic peak (peak 2) ending at 760°C, is due to the melting of Al. After heated to 820°C, carbon disappears, a very small amount of ZrO_2 remains in both samples, while Al_4C_3 and large amounts of $ZrAl_3$ phases are newly detected through XRD anal-

ysis (Figs 2b and 3b), suggesting that this exothermic peak involves the formation of the two new phases. In the corresponding microstructures (Figs 8a and 9a), only $ZrAl_3$ and some ZrO_2 are observed in the Al matrix. Al_4C_3 phase is absent because it readily reacts with H_2O, which is necessary during polishing the samples to obtain clear micrographs.

After P1 sample is heated to 960°C, peaks of $ZrAl_3$ and Al_4C_3 disappear and strong ones corresponding to Al_2O_3 and $Zr_2Al_3C_5$ are revealed in XRD (Fig. 2c). This is in agreement with the microstructure

Phase evolution during heating the 8 h milled Al-ZrO$_2$-C powder samples with different ZrO$_2$/C ratios (r) to different temperatures

	P1 ($r = 2:5$)	P2, P4 ($r = 3:4, 3:5$)	P3 ($r = 1:1$)
As milled	Al, ZrO$_2$, C	Al, ZrO$_2$, C	Al, ZrO$_2$, C
820°C	Al, ZrO$_2$, ZrAl$_3$, Al$_4$C$_3$,	Al, ZrO$_2$, ZrAl$_3$, Al$_4$C$_3$,	Al, ZrO$_2$, ZrAl$_3$, Al$_4$C$_3$,
960°C	Al, Al$_2$O$_3$, Zr$_2$Al$_3$C$_5$		
1000°C		Al, Al$_2$O$_3$, ZrAl$_3$, Zr$_2$Al$_3$C$_5$	Al, Al$_2$O$_3$, ZrAl$_3$, Zr$_2$Al$_3$C$_5$
1250°C	Al, Al$_2$O$_3$, Zr$_2$Al$_3$C$_5$,	Al, Al$_2$O$_3$, ZrAlC$_2$, ZrC	Al, ZrAl$_3$, Al$_2$O$_3$, ZrAlC$_2$, ZrC

observation (Fig. 8b and c), but at low magnification a minor amount of ZrAl$_3$ (under the detection limit of XRD analysis) can be observed (Fig. 8b). Further heating P1 sample to 1250°C results in no further phase changes (Fig. 2d, Fig. 8d and e), except that the small amount of ZrAl$_3$ disappears completely (Fig. 8d). In P2 sample heated to 1000°C, the intensity of XRD peaks of ZrAl$_3$ is greatly decreased, diffraction peaks of Al$_4$C$_3$ disappear, and strong ones corresponding to Zr$_2$Al$_3$C$_5$ and Al$_2$O$_3$ newly appear. It is clear from these observations in both P1 and P2 that the endothermic peak starting at 918°C corresponds to the formation of Zr$_2$Al$_3$C$_5$ from ZrAl$_3$ and Al$_4$C$_3$.

In the final product of P2 sample at 1250°C, ZrAl$_3$ and Zr$_2$Al$_3$C$_5$ phases, which are detected at 1000°C in XRD analysis, disappear completely, while ZrAlC$_2$ and ZrC are newly found (Fig. 3), i.e. the final product is a mixture of Al, ZrAlC$_2$, ZrC, and Al$_2$O$_3$. It can be concluded that the formation of ZrAlC$_2$ and ZrC phases from Zr$_2$Al$_3$C$_5$ and ZrAl$_3$ contributes to the endothermic peak at 1144°C (peak 5). In the corresponding microstructure (Fig. 9d), some ZrAl$_3$ is still observed at 1250°C. Apparently, the amount of ZrAl$_3$ is small and under the detection limit of the XRD analysis.

DSC curves of P3 and P4 samples show reaction peaks similar to those of P2 (Table I). Phases detected by XRD in P4 sample heated to different temperatures are the same as those of P2, while the phase evolution during heating P3 is slightly different from that of P2: a large amount of ZrAl$_3$ is still left in the final P3 product (Table II).

DSC curves of P5 and P6 samples are shown in Fig. 4. A comparison between Figs 1 and 4 indicates that lowering the heating rate from 20 to 5°C/min results in no changing of reaction events but some differences in reaction temperatures. The start of Al melting peak is
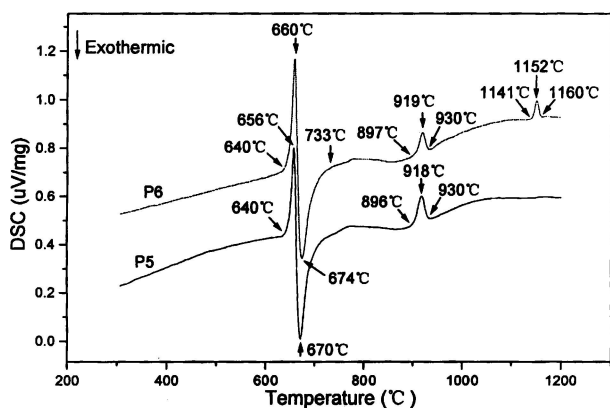
not changed, the start of peak 5 is only 3°C lower at 5°C/min than at 20°C/min, while larger decrease (20–25°C) of start temperatures occurs for both peak 2 and peak 4, suggesting strong kinetic dependence to the two reaction events.

3.2. Al-ZrO$_2$-C powders ball milled for 4 h
In addition to reaction events (peak 1, 2, 4, and/or 5) similar to those of P1 and P2, DSC curves of P7 and P8 exhibit a new exothermic peak (peak 3) which starts at 845°C and is closely connected with peak 4 (Fig. 5). It can be seen from the relevant XRD analysis of P7 sample (Fig. 6 and Table 3) that there are still a large amount of ZrO$_2$ remaining at 820°C, but this is decreased to a minor amount at 910°C, meanwhile the amount of ZrAl$_3$ is greatly increased after peak 3, clearly
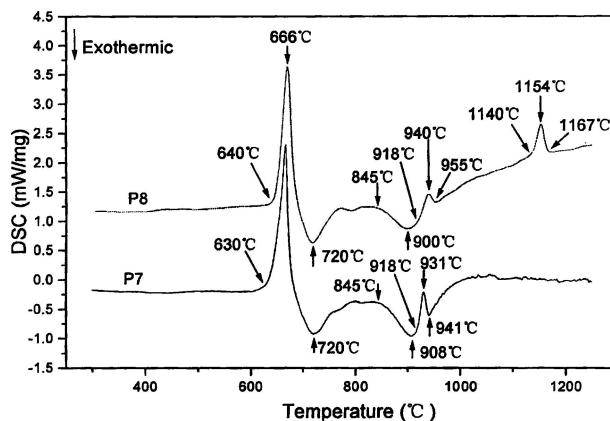

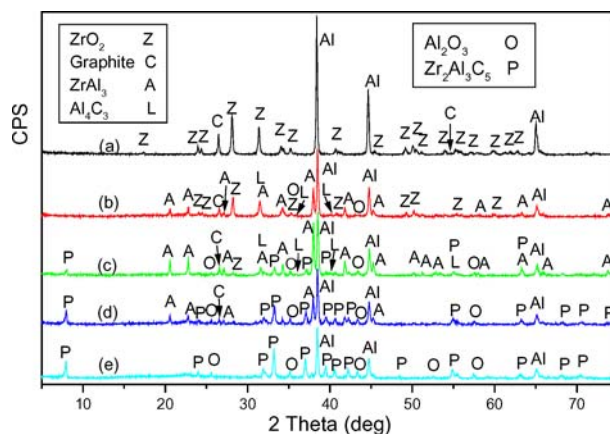*Figure 5* DSC traces of P7 and P8 samples.

Figure 6 X-ray diffraction patterns of P7 sample heated to different temperatures by DSC. (a) as milled powder; (b) 820°C; (c) 910°C; (d) 943°C; (e) 1250°C.

Figure 4 DSC traces of P5 and P6 samples.

	Phases detected
As milled	Al, ZrO_2, C
820°C	Al, ZrO_2, C, $ZrAl_3$, Al_4C_3, Al_2O_3
910°C	Al, ZrO_2, C, $ZrAl_3$, Al_4C_3, Al_2O_3, $Zr_2Al_3C_5$
943°C	Al, C, $ZrAl_3$, Al_4C_3, Al_2O_3, $Zr_2Al_3C_5$,
1250°C	Al, Al_2O_3, $Zr_2Al_3C_5$,
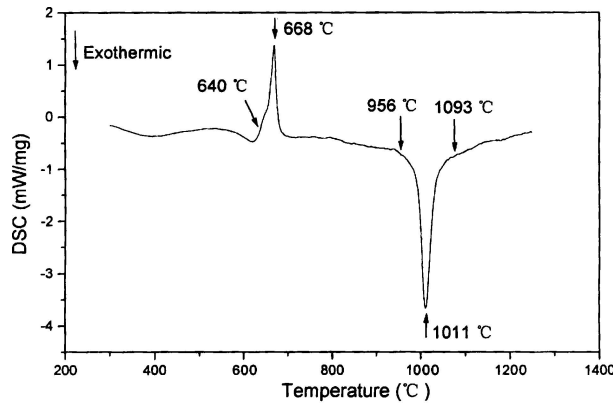
(a)
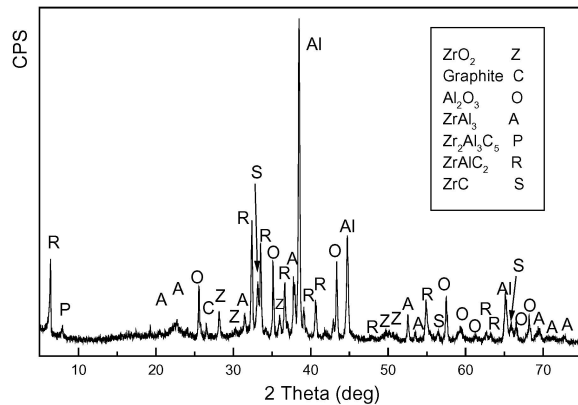
(b)

Figure 7 DSC trace of P9 sample heated to 1250°C (a), and corresponding XRD pattern of the final product (b).

suggesting that this exothermic event also involves the formation of $ZrAl_3$ from ZrO_2 and Al. In the XRD pattern of the starting powder of P7 (Fig. 6), the diffraction peaks of carbon are much stronger than those in 8 h milled P1- P4 samples (Figs 2 and 3), and at 820, 910, and 943°C there are still a small amount of carbon left, indicating that prolonged milling promotes mixing and enhances chemical reaction in the heating process.

3.3. Al-ZrO_2-C powder ball milled for 1 h
Except for the melting of Al, the DSC curve of P9 powder ball milled for an hour, Fig. 7a, shows a large exothermic peak around 956°C. The relevant XRD analysis reveals new appearances of the $ZrAlC_2$, ZrC, $ZrAl_3$, $Zr_2Al_3C_5$, Al_2O_3 phases, and some amounts of original ZrO_2, and carbon in the Al matrix. Apparently the reaction between the three starting materials occurs at this exothermic peak, forming the above new phases.

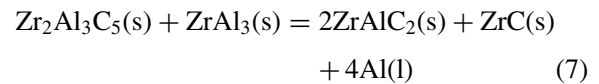## 4. Discussions
4.1. Reaction process
From above combined analyses during heating the 8 h milled P1-P6 samples through DSC, XRD, and EPMA, it can be deduced that the exothermic event soon after the melting of Al is the liquid Al reacting simultaneously with ZrO_2 and carbon particles to form $ZrAl_3$ and Al_4C_3 according to the following two equations, respectively.

$$4Al(l) + 3C(s) = Al_4C_3(s) \qquad (2)$$

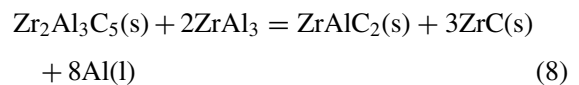$$13Al(l) + 3ZrO_2(l) = 3ZrAl_3(s) + 2Al_2O_3(s) \quad (5)$$
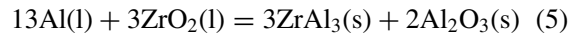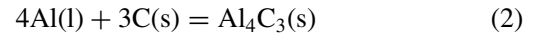
Neither XRD nor microstructure observation reveals the presence of Al_2O_3 phase at 820°C, while the X-ray mapping (Fig. 9b) suggests that O element is uniformly distributed in the Al matrix. It is possible that Al_2O_3 grains are too fine to be detected by either XRD or SEM. Then, at 896 or 918°C (peak 4) Al_4C_3 and $ZrAl_3$ react to form $Zr_2Al_3C_5$ phase:

$$6ZrAl_3(s) + 5Al_4C_3(s) = 3Zr_2Al_3C_5(s) + 29Al(l)$$
$$(6)$$
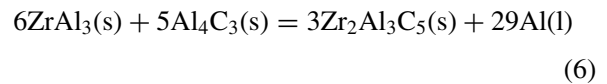
After this reaction, all the Zr and carbon contents in the Al-ZrO_2-C powders with ZrO_2/C molar ratio = 2:5 are transmitted into the $Zr_2Al_3C_5$ compound, which keeps stable in the final product heated to 1250°C. In the samples with ZrO_2/C molar ratios equal to 1:1, 3:4, and 3:5, $ZrAl_3$ is still excessive after reaction (6) is completed. Further heating to around 1140°C, two new carbides are formed from the reaction between $ZrAl_3$ and $Zr_2Al_3C_5$, according to:

$$Zr_2Al_3C_5(s) + ZrAl_3(s) = 2ZrAlC_2(s) + ZrC(s)$$
$$+ 4Al(l) \qquad (7)$$

or

$$Zr_2Al_3C_5(s) + 2ZrAl_3 = ZrAlC_2(s) + 3ZrC(s)$$
$$+ 8Al(l) \qquad (8)$$

The validity of exothermic reactions (2) and (5) have been further confirmed based on thermodynamic calculations [9, 10, 14]. However, it is impossible to verify the endothermic Equations 6–8 using the same method because thermodynamic data for $Zr_2Al_3C_5$ and $ZrAlC_2$ are unavailable at present. But they are strongly supported by a completely different experiment performed by Hashimoto *et al.* [15] during heating Al-ZrC powder mixture from room temperature to 1600°C: When heating at 800°C, large amounts of $ZrAl_3$ were present in the Al-ZrC mixture. A sudden decrease of the amount of $ZrAl_3$ phase and the new appearance of the $Zr_2Al_3C_5$ phase occurred at 900°C, agreeing well with the onset temperature of reaction (6), 896°C, when heating at the rate of 5°C/min, as suggested in Fig. 4. Between 1100 and 1200°C, the vanishing of the $Zr_2Al_3C_5$ phase, the appearance of the $ZrAlC_2$ and ZrC phases, and the increase of Al amount was observed in the mixture. This

is in good agreement with the present phase changes before and after the endothermic peak which starts at about 1140°C and ends at about 1174°C (Figs 1, 4, and 5), hence confirming the validity of reaction (7) or (8).

As will be discussed in the next section, $ZrAl_3$ formed from Al-ZrO_2 reaction at lower temperature dissolves in Al melt during further heating, it is reasonable to believe that reactions (6)–(8) proceed through the dissolved Zr reacting with Al_4C_3 and $Zr_2Al_3C_5$, respectively. Approximately 5 wt pct Zr is soluble in Al melt at 1140°C and only about 0.3 wt pct at 900°C [16], as the dissolved Zr reacts and is consumed, the solid $ZrAl_3$ particles dissolve. At 1140°C, not only the solubility of Zr is higher than that at 900°C, but also the diffusion rate of Zr solute in Al melt and the dissolving rate of $ZrAl_3$ particles are enhanced, so the solid $Zr_2Al_3C_5$ in Al melt is always in contact with sufficient Zr solute, and the reaction (7) or (8) readily proceeds around its equilibrium reaction temperature (about 1140°C as suggested by Figs 1, 4, 5) at both heating rates. At about 900°C, however, Zr solute in the liquid Al is limited, the process of reaction (6) is mainly dominated by the dissolving rate of $ZrAl_3$ and the diffusion of Zr solute towards Al_4C_3 particle. Lower heating rate means longer time for sufficient Zr solute to diffuse towards Al_4C_3 in a fixed temperature range, whereas at higher heating rate, sufficient Zr for reaction (6) to proceed is only available at some higher temperature point, thus causing the deviation from equilibrium reaction temperature. A similar effect of heating rate also occurs for the Al-ZrO_2 and Al-C reactions (Equations 2 and 5), but in these cases, the kinetics are likely to be mainly determined by the diffusion rates of Al, Zr, and C through the oxide film on the Al particle surfaces.

When the milling time decreases to 4 h, reactions (6)–(8) do not change, while reactions (2) and (5) proceed in two steps: one starts soon after the melting of Al and the other at about 845°C, as evident in Fig. 5. In the powder milled for only an hour (Fig. 7), it is considered that the following reactions occur corresponding to the large exothermic peak:

$$3ZrO_2 + 4C + 5Al = ZrAlC_2 + 2ZrC + 2Al_2O_3 \quad (9)$$

$$3ZrO_2 + 5C + 5Al = 2ZrAlC_2 + ZrC + 2Al_2O_3 \quad (10)$$
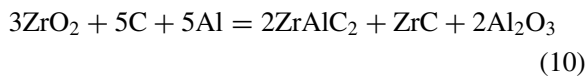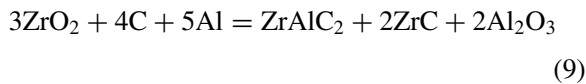
According to the ZrO_2/C ratio (2:5) in the starting P9 powder, the final product should be a mixture of Al, $Zr_2Al_3C_5$ and Al_2O_3. Due to the poor contacting/wetting of ZrO_2 and carbon particles with Al particle, part of the original carbon and ZrO_2 do not take part in the reaction, thus changing the Zr/C ratio in the new compounds of the final product. From the sum of reactions (2), (5), (6), the following equation is obtained:
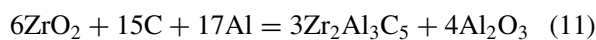
$$6ZrO_2 + 15C + 17Al = 3Zr_2Al_3C_5 + 4Al_2O_3 \quad (11)$$

TABLE IV Phases obtained after heating the Al-ZrO_2-C system with different ZrO_2/C molar ratios to 1250°C

r	Final phases in the Al-ZrO_2-C system after heated to 1250°C
$r > 3{:}4$	Al, $ZrAl_3$, ZrC, $ZrAlC_2$, Al_2O_3
$3{:}5 \le r \le 3{:}4$	Al, ZrC, $ZrAlC_2$, Al_2O_3
$2{:}5 < r < 3{:}5$	Al, ZrC, $ZrAlC_2$, $Zr_2Al_3C_5$, Al_2O_3
$r = 2{:}5$	Al, $Zr_2Al_3C_5$, Al_2O_3
$r < 2{:}5$	Al, $Zr_2Al_3C_5$, Al_2O_3, Al_4C_3

It is supposed that if all the ZrO_2 and carbon in P9 sample participated in the reaction, the above reaction would have occurred.

From a combination of formulae (9)–(11) and final phases present in the Al-ZrO_2-C systems with above critical ZrO_2/C molar ratios (Table II), phases obtained in the Al matrix after heating the Al-ZrO_2-C systems with different ZrO_2/C ratios to 1250°C are concluded and listed in Table IV.

From the present phase evolution during heating Al-ZrO_2-C powders in DSC and that found in ref. [15] during sintering Al-ZrC mixture, it is clear that ZrC is instable in Al: it reacts with Al to form $ZrAl_3$ and Al_4C_3 soon after the Al melts, $ZrAl_3$ and $Zr_2Al_3C_5$ between 896 and 1140°C, or $ZrAlC_2$ above 1140°C. Thus, it is impossible to obtain aluminum composite reinforced with ZrC and Al_2O_3 particles through heating the Al-ZrO_2-C system to 1250°C.

4.2. Microstructure evolution

It can be seen from Figs 8 and 9 that the $ZrAl_3$ phase mainly presents flaky morphology at 820°C, but blocky form at 1000 and 1250°C. Its size increases with the rise of temperature, but there are still a small amount exhibiting flaky shape at high temperatures. The changes of $ZrAl_3$ morphology and size indicate that there has been the dissolution, re-nucleation and growth of $ZrAl_3$ during the heating process. It was reported that $ZrAl_3$ morphology is influenced by the combined effects of temperature, cooling rate, and composition [17]: high temperature, fast cooling rate, and the location of the composition in the liquid area favor the formation of flaky morphology, while low temperature, low cooling rate, the location of the composition in the solid-liquid area the blocky form. The presence of flaky morphology at 820°C but blocky type at 1000 and 1250°C in the present study seems to contradict this. It is thought that large amount of heat released from the reaction between ZrO_2 and Al is not transmitted to the surrounding area in time and largely increases the local temperature of the reaction zone, leading to the high-temperature characteristic of $ZrAl_3$. During further heating, $ZrAl_3$ dissolves, re-nucleates and grow in blocky morphology. When cooled from higher temperature, there will be longer time and faster diffusion rate of Zr in Al melt for the growth of $ZrAl_3$ particle, leading to the larger particle size at higher temperature (Fig. 9c and d).

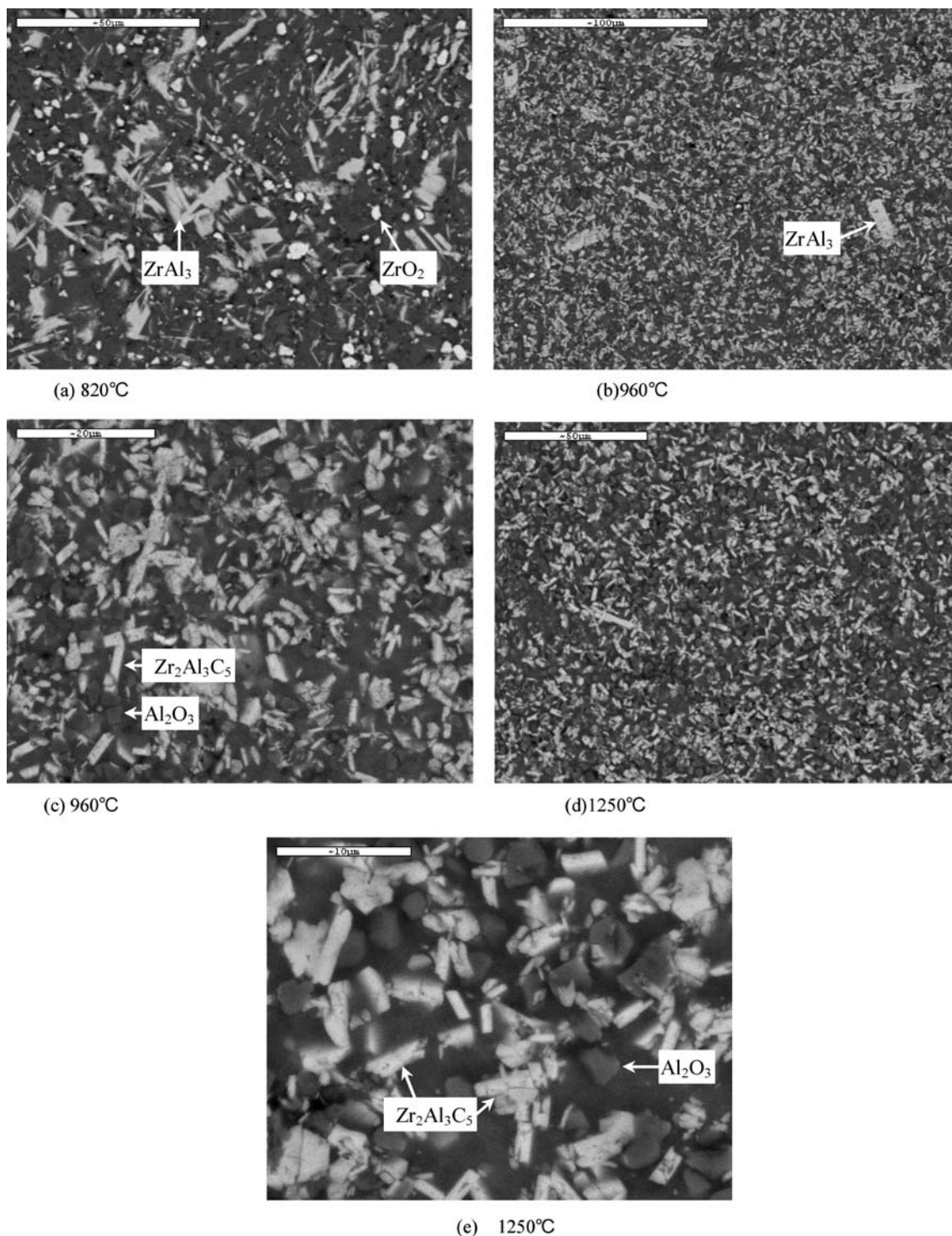Figs 8b–e and 9c show that $Zr_2Al_3C_5$ compound in both samples presents platelet morphology with the

Figure 8 Micrographs of P1 sample heated to different temperatures.

length ranging between 1.3–5 μm and width between 0.2–1.5 μm. The ZrAlC$_2$ and ZrC particles of 0.4–4 μm in size in the final P2 sample (Fig. 9e) present polygonal shape. Some relatively large particles (>2 μm) are precisely identified to be ZrAlC$_2$ through EDS quantitative analysis, but no ZrC has been determined this way. It is possible that ZrC particle is so small in size, being similar to or under that of the diameter of the electron beam of EPMA (about 1 μm), that the Al from the matrix is also detected in the EDS analysis, causing the difficulty of distinguishing it from ZrAlC$_2$ phase.

4.3. Effect of ball milling on the reaction process

It is clear that ball milling has a significant effect on the reaction process within the Al-ZrO$_2$-C system. There are two reaction modes during heating the Al-ZrO$_2$-C powders milled for different times: one-step reaction in the 1 h milled powder, wherein the three original phases react at a relatively high temperature, directly resulting in the ultimate products, as suggested by Equations 9–11, and multi-step reaction in the 4 and 8 h milled powders, which proceeds through Al reacting with ZrO$_2$/C at lower temperatures and the intermediate
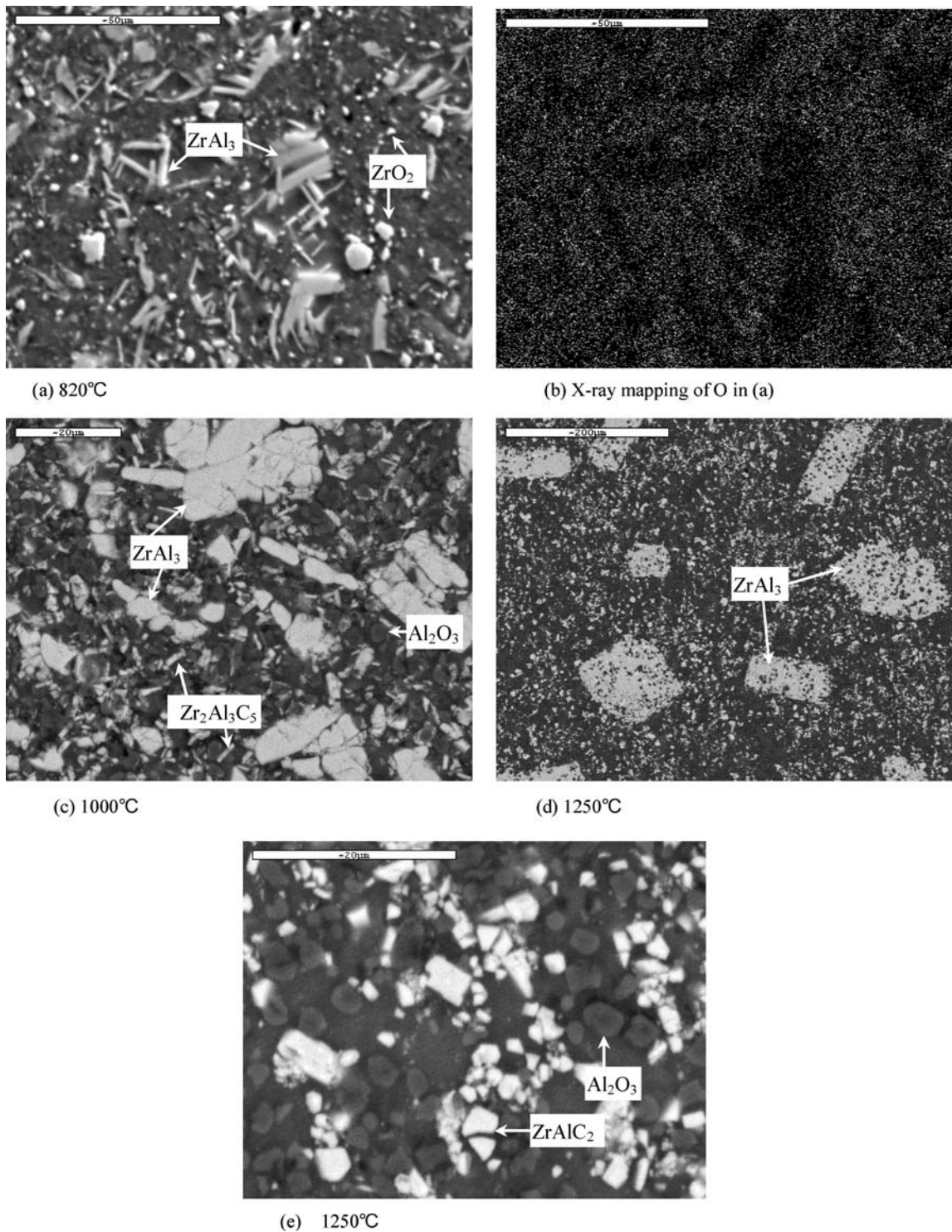
Figure 9 Micrographs of P2 sample heated to different temperatures.

resultants reacting with each other during further heating (Equations 2, 5–8).

It has been well established [18] that ball milling of powder reactants can significantly decrease the temperature needed to activate the reaction thermally, which is mainly attributed to the following three factors: reduction of the particle size, increase of the interfacial area between reactants, enhancement of the atomic diffusivity due to the introduction of a large concentration of defects such as dislocations and grain boundaries. It is believed that the 1 h milled powder was not fully mixed and the contact area between particles is smaller compared with the 4 and 8 h milled ones. During heating, the reaction is mainly controlled by the elemental diffusion at the inter-particle points. The reaction between Al and ZrO_2/C does not occur until the diffusion rate is sufficiently enhanced at a high temperature. Once the reactions start, the heat released further causes the large rise of the local temperature, enhancing the diffusion rate and leading to an overall exothermic reaction between the three starting phases as shown in Equations 9–11.

The powders ball milled for 8 and 4 h are intimately mixed, thus giving a much larger contact area
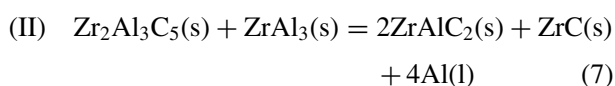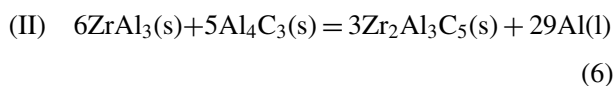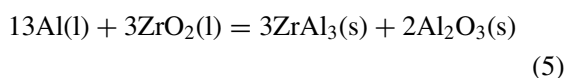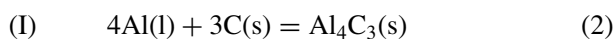
between Al and the other two particles. ZrO_2 and carbon particles are fully surrounded by aluminum particles, allowing the simultaneous diffusion in all directions rather than the point contact as in the 1 h milled powder. In addition, the reduced particle size shortens diffusion paths, resulting in less time taken for the diffusion from the center of particles in the 8 and 4 h milled powder than in the 1 h milled one. Thus, the rate of reactions between Al and ZrO_2/C is greatly enhanced at lower temperatures. Because the matrix temperature is low, the heat given out by the Al-ZrO_2 and Al-C reactions is not enough to increase the temperature to points at which the endothermic reactions (6)–(8) occur, so the reaction path in the 8 h and 4 h milled powders presents step-by-step characteristic during the heating process.

In the 4 h milled powder, the Al-ZrO_2 reaction is completed in two steps instead of one step as in the 8 h milled powder. One reason might be that the sizes of ZrO_2 and carbon particles with shorter milling time are not sufficiently reduced so that $ZrAl_3$ and Al_4C_3 formed in the interfacial area separate the remaining ZrO_2/C and Al particles and hinder the atomic diffusions, leading to the need of heating the powder to a higher temperature to further activate the reactions as a second step. Another possibility is that part of the ZrO_2/C particles in the 4 h milled powders are reduced to especially small sizes and fully mixed with the Al particles and completely reacts with Al at a lower temperature (the first step), while another part has relatively larger particle sizes and are in poor contact with Al and the reactions occur only at a higher temperature (the second step).
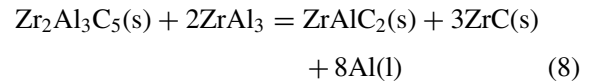
5. Conclusions

The reaction process in the ball milled ($50\text{gAl} + 18.6\text{gZO}_2 + x\text{gC}$) powder mixtures, where x is varied to obtain different ZrO_2/C molar ratios, have been studied by using a combination of DSC, XRD, and EPMA, the following results can be obtained:
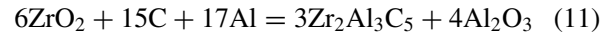
(1) During heating the Al-ZrO_2-C powders fully mixed through ball milling for 8 h, the Al first melts, then reacts simultaneously with ZrO_2 and carbon particles to form $ZrAl_3$ and Al_4C_3 phases, which further react with each other at about 896°C, forming $Zr_2Al_3C_5$. At about 1140°C, $Zr_2Al_3C_5$ reacts with $ZrAl_3$, producing ZrC and $ZrAlC_2$ phases; if there is not excessive $ZrAl_3$ for the reaction to proceed, $Zr_2Al_3C_5$ is stable in the Al melt heated to 1250°C. The reaction process can be described as following equations:

$$(I) \qquad 4Al(l) + 3C(s) = Al_4C_3(s) \qquad (2)$$

$$13Al(l) + 3ZrO_2(l) = 3ZrAl_3(s) + 2Al_2O_3(s) \qquad (5)$$

$$(II) \quad 6ZrAl_3(s) + 5Al_4C_3(s) = 3Zr_2Al_3C_5(s) + 29Al(l) \qquad (6)$$

$$(II) \quad Zr_2Al_3C_5(s) + ZrAl_3(s) = 2ZrAlC_2(s) + ZrC(s) + 4Al(l) \qquad (7)$$

or

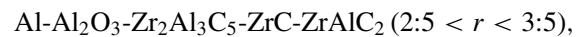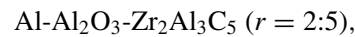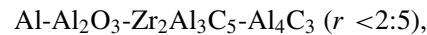$$Zr_2Al_3C_5(s) + 2ZrAl_3 = ZrAlC_2(s) + 3ZrC(s) + 8Al(l) \qquad (8)$$

When the powder is not fully mixed (ball milled for 1 h), only an exothermic reaction between the three original phases occurs at higher temperature to form $Zr_2Al_3C_5$ according to:

$$6ZrO_2 + 15C + 17Al = 3Zr_2Al_3C_5 + 4Al_2O_3 \quad (11)$$

or $ZrAlC_2$ and ZrC as the following:

$$3ZrO_2 + 4C + 5Al = ZrAlC_2 + 2ZrC + 2Al_2O_3 \quad (9)$$

$$3ZrO_2 + 5C + 5Al = 2ZrAlC_2 + ZrC + 2Al_2O_3 \quad (10)$$

(2) Through heating Al-ZrO_2-C powders with different ZrO_2/C molar ratios (r) to 1250°C, Al alloys embedded with different phases are obtained:

Al-Al_2O_3-$Zr_2Al_3C_5$-Al_4C_3 ($r < 2:5$),

Al-Al_2O_3-$Zr_2Al_3C_5$ ($r = 2:5$),

Al-Al_2O_3-$Zr_2Al_3C_5$-ZrC-$ZrAlC_2$ ($2:5 < r < 3:5$),

Al-Al_2O_3-ZrC-$ZrAlC_2$ ($3:5 \leq r \leq 3:4$),

Al-$ZrAl_3$-Al_2O_3-ZrC-$ZrAlC_2$ ($r > 3:4$).

Thus, it is not feasible to obtain ZrC and Al_2O_3 particulate reinforced Al composite from this system. But the above alloys might be new potent composite materials, and need to be further studied.

(3) $ZrAl_3$ present flaky morphology after it is produced from Al-ZrO_2 reaction at lower temperature, but blocky form at higher temperature, and the size increases with the increase of the temperature experienced. $Zr_2Al_3C_5$ compound presents fine platelet morphology, and $ZrAlC_2$ and ZrC polygonal shape.

References
1. A. O. KUNRATH, T. R. STROHAECKER and J. J. MOORE, *Scripta Materialia* **34** (1996) 189.
2. L. LÜ, M. O. LAI, Y. SU, *et al., ibid.* **45** (2001) 1017.
3. YUYONG CHEN and D. D. L. CHUNG, *J. Mater. Sci.* **36** (1995) 4609.
4. X. C. TONG, *ibid.* **33** (1998) 5365.
5. SUBHASH KHATRI and MICHAEL KOCZAK, *Mater. Sci. Engng. A* **162** (1993) 153.
6. M. K. PREMKUMAR and M. G. CHU, *ibid.* **202** (1995) 172.
7. T. TAKIDA, M. MABUCHI, M. NAKAMUR, *et al., ibid.* **276** (2000) 269.
8. P. C. MAITY, S. C. PANIGRAHI and P. N. CHAKRABORTY, *Scripta Metall. Mater.* **28** (1993) 549.
9. Y. ZHAO, Ph.D Thesis, Southeastern University, P.R. China, June 2001.

10. W. DEQING, J. NEUMANN and H. F. LÓPEZ, *Metall. Mater. Trans. A* **34** (2003) 1357.
11. ZHENQING WANG, XIANGFA LIU, JUNYAN ZHANG and XIUFANG BIAN, *J. Mater. Sci.* **39** (2004) 667.
12. ZHENQING WANG, XIANGFA LIU and XIUFANG BIAN, A Method to Prepare Aluminum Alloys Containing TiC and Al_2O_3 Ceramic Particles, China Patent, No. 200310105445.8
13. Q. J. ZHENG and R. G. REDDY, *High Temp. Mater. Proc.* **22** (2003) 35.
14. ROBERT A. RAPP and XUEJIN ZHENG, *Metall. Trans.* **22A** (1991) 3071.
15. SHINOBU HASHIMOTO and AKIRA YAMAGUCHI, *J. Mater. Sci.* **33** (1998) 4835.
16. J. MURRAY, A. PERUZZI and J. P. ABRIATA, *J. Phase Equilibria* **13** (1992) 277.
17. M. S. LEE and B. S. TERRY, *Mater. Sci. Techn.* **7** (1991) 608.
18. D. L. ZHANG and D. Y. YING, *Mater. Sci. Engng.* **A301** (2001) 90.